

Cross sections of the $^{144}\text{Sm}(n,\alpha)^{141}\text{Nd}$ and $^{66}\text{Zn}(n,\alpha)^{63}\text{Ni}$ reactions at 4.0, 5.0 and 6.0 MeV

Gledenov Yury^{1,a}, Zhang Guohui², Gonchigdorj Khuukhenkhuu³, Sedysheva Milana¹, Krupa Lubos^{4,5}, Enkhbold Sansarbayar¹, Chuprakov Igor¹, Wang Zhimin², Fan Xiao², Zhang Luyu², and Bai Huaiyong²

¹ Frank Laboratory of Neutron Physics, Joint Institute for Nuclear Research, Dubna 141980, Russia

² State Key Laboratory of Nuclear Physics and Technology, Institute of Heavy Ion Physics, Peking University, Beijing 100871, China

³ Nuclear Research Centre, National University of Mongolia, Ulaanbaatar, Mongolia

⁴ Flerov Laboratory of Nuclear Reactions, Joint Institute for Nuclear Research, Dubna 141980, Russia

⁵ Institute of Experimental and Applied Physics, Czech Technical University in Prague, Horska

Abstract. Cross sections of the $^{144}\text{Sm}(n,\alpha)^{141}\text{Nd}$ and $^{66}\text{Zn}(n,\alpha)^{63}\text{Ni}$ reactions were measured at $E_n = 4.0, 5.0$ and 6.0 MeV performed at the 4.5-MV Van de Graaff Accelerator of Peking University, China. A double-section gridded ionization chamber was used to detect the alpha particles. The foil samples of $^{144}\text{Sm}_2\text{O}_3$ and enriched ^{66}Zn were placed at the common cathode plate of the chamber. Monoenergetic neutrons were produced by a deuterium gas target through the $^2\text{H}(d,n)^3\text{He}$ reaction. The neutron flux was monitored by a BF_3 long counter. Cross sections of the $^{238}\text{U}(n,f)$ reaction were used as the standard to perform the (n,α) reaction measurement. Present results are compared with existing measurements and evaluations. They are generally in agreement with TALYS-1.6 code calculations. For the $^{144}\text{Sm}(n,\alpha)^{141}\text{Nd}$ reaction our measurements support the data of JEF-2.2. For the $^{66}\text{Zn}(n,\alpha)^{63}\text{Ni}$ reaction present results support the data of EAF-2010 and TENDL-2015 data.

1. Introduction

Cross section data for the charged particle emitted reactions induced by the fast neutron are important both in basic nuclear physics and nuclear engineering applications. Samarium isotopes are relatively high-yield fission products in nuclear reactors and zinc is one of the structural materials for nuclear reactors and other high energy installations, so accurate knowledge of their neutron cross sections can be important for nuclear technology applications. The (n,α) reactions, in particular, are gas-producing and exothermic ones. The helium gas accumulated in the material will cause [1] serious embrittlement problems. Experimental measurements, however, are rather scanty for $^{144}\text{Sm}(n,\alpha)^{141}\text{Nd}$ and $^{66}\text{Zn}(n,\alpha)^{63}\text{Ni}$ reactions. For the $^{144}\text{Sm}(n,\alpha)^{141}\text{Nd}$ reaction, only two measurements exist for neutron energies around 14 MeV, and there are large differences between them [2]. For the $^{66}\text{Zn}(n,\alpha)^{63}\text{Ni}$ reaction, no measurements were made for neutron energies from 0 to 20 MeV. Although most of evaluated nuclear data libraries contain these two reactions, large discrepancies exist among them both in the trend and magnitude [3]. So, accurate measurements are demanded to address the application needs and clarify exciting discrepancies among different libraries.

We have measured the cross sections of the $^{147}\text{Sm}(n,\alpha)^{144}\text{Nd}$ reaction at $E_n = 5.0$ and 6.0 MeV, the $^{149}\text{Sm}(n,\alpha)^{146}\text{Nd}$ reaction at $E_n = 4.5, 5.0, 5.5, 6.0$ and 6.5 MeV [4]. The (n,α) reaction cross sections for zinc

isotopes we have measured contain the $^{64}\text{Zn}(n,\alpha)^{61}\text{Ni}$ reaction at $E_n = 2.5, 4.0, 5.0, 5.5$ and 6.0 MeV and the $^{67}\text{Zn}(n,\alpha)^{64}\text{Ni}$ reaction at $E_n = 4.0, 5.0$ and 6.0 MeV [5,6]. In the present work, we measured the $^{144}\text{Sm}(n,\alpha)^{141}\text{Nd}$ and $^{66}\text{Zn}(n,\alpha)^{63}\text{Ni}$ reactions at $E_n = 4.0, 5.0$ and 6.0 MeV.

2. Details of experiments

The experiments were performed at the 4.5-MV Van de Graaff accelerator of Peking University, China. The experimental apparatus consists of three main parts: the neutron source, the charged particle detector (with samples inside) and the neutron flux monitor.

A deuterium gas target was used to produce the monoenergetic neutron through the $^2\text{H}(d,n)^3\text{He}$ reaction.

The α -particle detector is a double-section gridded ionization chamber (GIC) with a common cathode, and its structure can be found in Ref. [7]. Working gas of the GIC was Kr + 2.83% CO_2 .

In the present work, enriched $^{144}\text{Sm}_2\text{O}_3$ and ^{66}Zn foil samples were prepared. The foil samples were prepared using the press method with which nearly all material can be utilized without loss. Data of the samples are listed in Table 1.

A sample changer was set at the common cathode of the ionization chamber with five sample positions, and back-to-back double samples can be placed at each of them [7]. The $^{144}\text{Sm}_2\text{O}_3$ and enriched ^{66}Zn foil samples were attached to the tantalum backings 0.1 mm in thickness. With back-to-back samples, forward ($0^\circ \sim 90^\circ$) and backward ($90^\circ \sim 180^\circ$) emitted α -particles can be detected simultaneously.

^a e-mail: ygledenov@gmail.com

Table 1. Description of the samples.

Samples	Abundance (%)	Thickness ($\mu\text{g}/\text{cm}^2$)	Diameter (mm)
^{144}Sm	95.0	4300 ^a and 3370 ^b	44.0 ^a and 44.0 ^b
^{66}Zn	98.7	723 ^a and 708 ^b	43.0 ^a and 47.0 ^b
^{238}U	99.999	493.6	45.0

^a Forward sample. ^b Backward sample.

A ^{238}U sample was placed in the GIC at the forward direction of the other positions of the sample changer to determine the absolute neutron flux by measuring the fission fragments.

The neutron flux monitor is a BF_3 long counter. The axis of the counter was along the normal line of the electrodes of the ionization chamber as well as the 0° direction of the deuteron beam line.

Two-dimensional spectra of the cathode-anode coincidence signals for forward and backward directions were recorded separately, from which the number of α -events from the measured (n,α) reactions can be obtained. The data-acquisition system (DAQS) can be found in Ref. [8]. Generally, for each neutron energy point, the experimental process in turn is as follows: 1) compound α source measurement for energy calibration of the DAQS, 2) foreground measurement for expected α events, 3) background measurement with tantalum sheets, 4) ^{238}U fission fragment measurement for neutron flux calibration with the BF_3 long counter, and 5) α source measurement again for checking the stability of the DAQS. However, because the Q value of the $^{144}\text{Sm}(n,\alpha)^{141}\text{Nd}$ reaction is relatively large (7.874 MeV) comparing with that of the background reaction, the background measurement had not been done for the $^{144}\text{Sm}(n,\alpha)^{141}\text{Nd}$ reaction. At neutron energy point $E_n = 4.0, 5.0$ and 6.0 MeV, the beam duration was 46, 31 and 26 h, respectively for $^{144}\text{Sm}(n,\alpha)^{141}\text{Nd}$ reaction and 29, 16, 12 h for $^{66}\text{Zn}(n,\alpha)^{63}\text{Ni}$ reaction.

Since the $^{238}\text{U}(n,f)$ reaction were used as the standard to perform the measurement, the cross section σ of the (n,α) reaction can be calculated by the following equation:

$$\sigma = \sigma_f \cdot \frac{N_\alpha / \varepsilon_\alpha \cdot N_{238\text{U}} \cdot N_{\text{BF}_3-f}}{N_f / \varepsilon_f \cdot N_{\text{samp}} \cdot N_{\text{BF}_3-\alpha}} \quad (1)$$

The σ_f is the standard $^{238}\text{U}(n,f)$ cross sections taken from ENDF/B-VII.1 library [3]. The N_α and N_f are the detected counts above the energy threshold from the (n,α) reaction (after background subtraction) and from the $^{238}\text{U}(n,f)$ reaction, respectively. The ε_α and ε_f are the detection efficiency for α -particles and fission fragments. The $N_{238\text{U}}$ and N_{samp} are the numbers of ^{238}U and ^{144}Sm (or ^{66}Zn) nuclei in the samples, respectively, N_{BF_3-f} and $N_{\text{BF}_3-\alpha}$ are the counts of the neutron flux monitor (BF_3 counter) for ^{238}U fission and for (n,α) event measurements, respectively.

The detection efficiency for α -particles ε_α and fission fragments ε_f can be written as

$$\varepsilon = N_{\text{det}} / (N_{\text{det}} + N_{\text{th}} + N_{\text{ab}}) \quad (2)$$

Where N_{det} is the detected counts, i.e., N_α or N_f , N_{th} is the number of events with amplitudes below threshold (the threshold correction), and N_{ab} is the number

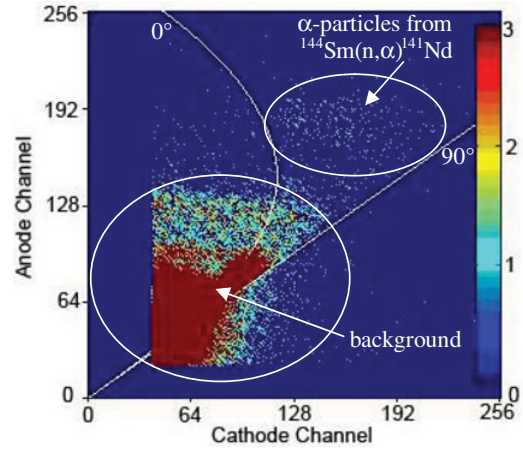


Figure 1. Two-dimensional spectrum of the $^{144}\text{Sm}(n,\alpha)^{141}\text{Nd}$ reaction at $E_n = 4.0$ MeV for the forward direction. The axes represent the amplitudes of cathode and anode signals of event.

of events absorbed in the samples (the self-absorption correction) [9]. The calculation method of ε will be discussed in the next section.

The cross sections of the $^{144}\text{Sm}(n,\alpha)^{141}\text{Nd}$ and $^{66}\text{Zn}(n,\alpha)^{63}\text{Ni}$ reactions in forward and backward directions can be calculated separately using Eqs. (1) and (2). The complete cross section can be obtained by adding them up together.

3. Data processing, results, and discussions

The data processing methods are almost the same for both (n,α) reactions to be measured at all neutron energies. As an example, the following descriptions are given for the data processing of the $^{144}\text{Sm}(n,\alpha)^{141}\text{Nd}$ at $E_n = 4.0$ MeV and $^{66}\text{Zn}(n,\alpha)^{63}\text{Ni}$ reactions at $E_n = 5.0$ MeV for the forward direction.

Firstly, a two-dimensional spectrum of compound α -sources was obtained and used for energy calibration and valid-event-area determination. The four groups of α particles, i.e., $\alpha_1, \alpha_2, \alpha_3, \alpha_4$ are emitted from $^{234}\text{U}, ^{239}\text{Pu}, ^{238}\text{Pu}$ and ^{244}Cm alpha sources with energies of 4.775, 5.155, 5.499, 5.805 MeV, respectively. The determined valid-event-area is between curves of the 0° and 90° emitted angle of α -particles as shown in Fig. 1.

Secondly, cathode-anode two-dimensional spectra for the foreground and background are obtained from the experimental data. As mentioned before, due to the large Q value background measurement for the $^{144}\text{Sm}(n,\alpha)^{141}\text{Nd}$ reaction were not made as shown in Fig. 1.

Figure 2 shows the results of $^{66}\text{Zn}(n,\alpha)^{63}\text{Ni}$ reaction after background subtraction. The valid-event-area was used to pick out the expected α -events from the $^{144}\text{Sm}(n,\alpha)^{141}\text{Nd}$ or $^{66}\text{Zn}(n,\alpha)^{63}\text{Ni}$ reactions.

Figures 3 and 4 show the anode spectrum after the projection of the selected α -events. As can be seen from the blue curves (pure event), α -events corresponding to different energy levels of the residual nuclei cannot be separated and they become one broad peak due to the close energy levels of the residual nuclei and the energy loss of α -particles in the sample. The α counts above the threshold can be obtained from the anode spectrum. The threshold are shown as the arrows in Figs. 3 and 4.

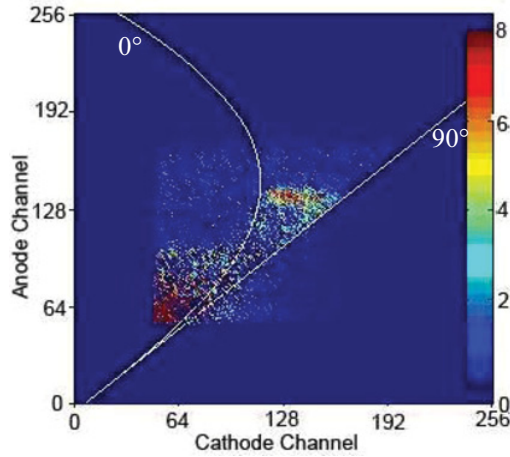


Figure 2. Two-dimensional spectrum of the $^{66}\text{Zn}(n,\alpha)^{63}\text{Ni}$ reaction at $E_n = 5.0$ MeV for the forward direction (after background subtraction).

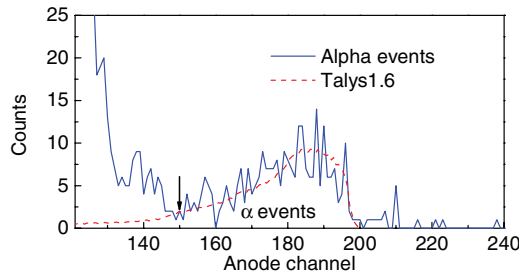


Figure 3. Anode spectrum of the $^{144}\text{Sm}(n,\alpha)^{141}\text{Nd}$ reaction at $E_n = 4.0$ MeV for the forward direction.

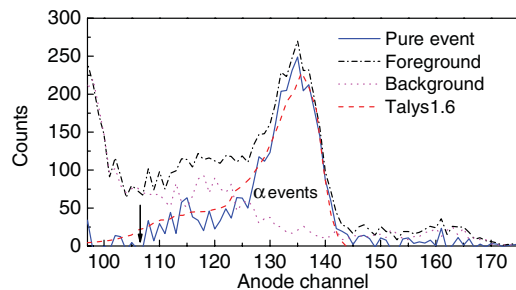


Figure 4. Anode spectrum of the $^{66}\text{Zn}(n,\alpha)^{63}\text{Ni}$ reaction at $E_n = 5.0$ MeV for the forward direction.

As shown in Figs. 3 and 4, in addition to the α counts above threshold, there are also α events below the threshold which cannot be detected. Therefore, threshold and self-absorption corrections are needed. To determine the detection efficiency of α -particle, the anode spectra were simulated as shown in Figs. 3 and 4 with the red curves. The SRIM code was used to get the stopping power of α -particles in the samples, and the TALYS-1.6 code to predict the angular and energy distributions of the emitted α -particles [10, 11]. To obtain the well fitted anode spectrum, level densities from Hilaire's combinatorial tables (Idmodel 5 in TALYS) were used within the TALYS-1.6 code to predict the angular and energy distributions of the emitted α -particles for the $^{144}\text{Sm}(n,\alpha)^{141}\text{Nd}$ reaction. For the $^{66}\text{Zn}(n,\alpha)^{63}\text{Ni}$ reaction, the default level densities, constant temperature model (Idmodel 1 in TALYS), were used.

Table 2. Measured and Talys-1.6 calculated cross sections for the $^{144}\text{Sm}(n,\alpha)^{141}\text{Nd}$ and $^{66}\text{Zn}(n,\alpha)^{63}\text{Ni}$ reactions.

E_n (MeV)	^{144}Sm		^{66}Zn	
	$\sigma_{\text{exp}}(\text{mb})$	$\sigma_{\text{Talys}}(\text{mb})$	$\sigma_{\text{exp}}(\text{mb})$	$\sigma_{\text{Talys}}(\text{mb})$
4.0	0.06 ± 0.01	$0.11^{\text{i}}, 0.08^{\text{ii}}$	1.80 ± 0.21	$1.13^{\text{i}}, 1.31^{\text{ii}}$
5.0	0.11 ± 0.03	$0.15^{\text{i}}, 0.11^{\text{ii}}$	5.45 ± 0.49	$4.02^{\text{i}}, 4.70^{\text{ii}}$
6.0	0.17 ± 0.03	$0.22^{\text{i}}, 0.17^{\text{ii}}$	10.0 ± 0.89	$9.38^{\text{i}}, 10.8^{\text{ii}}$

ⁱ Predictions of TALYS-1.6 with default parameters.

ⁱⁱ Predictions of TALYS-1.6 with adjusted parameters.

The corrected α counts are obtained through the division of α counts above threshold and the correction factor, which is calculated through the simulated anode spectra. The calculated correction factor value for the $^{144}\text{Sm}(n,\alpha)^{141}\text{Nd}$ reaction is from 77% to 82% and that for the $^{66}\text{Zn}(n,\alpha)^{63}\text{Ni}$ reaction is from 82% to 87%.

The measured results of cross sections for the $^{144}\text{Sm}(n,\alpha)^{141}\text{Nd}$ and $^{66}\text{Zn}(n,\alpha)^{63}\text{Ni}$ reactions are listed in Table 2. The calculated results using the TALYS-1.6 code with default and adjusted parameters are also listed in Table 2. Parameters of the optical model potential were adjusted to obtain a good agreement with present results. For the $^{144}\text{Sm}(n,\alpha)^{141}\text{Nd}$ reaction, the factor of geometry radius parameter, r_v , were adjusted from 1 (the default) to 0.8 and the constant c of the adjustment function for tabulated level densities were adjusted from 1 (the default) to 0.3. The adjustable range of the parameter r_v and c is from 0.1 to 10 and from -10 to 10 , respectively. Although the adjustments of the parameter r_v and constant c for tabulated level densities are in the adjustable range, they are relatively large. This may due to the fact that the ^{144}Sm is heavy nucleus and special structure may exist in the level densities. For the $^{66}\text{Zn}(n,\alpha)^{63}\text{Ni}$ reaction, the r_v were adjusted from 1 to 1.02 [11].

The uncertainty was calculated using the error propagation formula. Major source of uncertainty is the counting error for α particles (including statistics and background subtraction) produced by the valid-event-area cut and the energy threshold cut. The uncertainty of detection efficiency for α particles are due to the threshold and self-absorption correction based on Talys-1.6 code. Numbers of ^{144}Sm , ^{66}Zn nuclei were determined by the mass weighing. Numbers of ^{238}U nuclei were determined by α decay and the uncertainty of the numbers of nuclei is less than one percent.

Results of the present work are compared with those of existing measurements, evaluations, and TALYS-1.6 calculations as shown in Figs. 5 and 6. For the $^{144}\text{Sm}(n,\alpha)^{141}\text{Nd}$ reaction, there are large deviations among different evaluation libraries in the MeV region. Our measurements support the data of JEF-2.2 libraries. With the parameters adjustment, The TALYS-1.6 calculations agree with our measurements. Further measurements at neutron energies about 10 MeV and with other samarium isotopes are necessary to study the optical model parameters and level densities of the samarium nuclei.

Further measurements at neutron energies about 10 MeV are necessary to clarify the discrepancies among different libraries. For the $^{66}\text{Zn}(n,\alpha)^{63}\text{Ni}$ reaction as shown in Fig. 6, no measurements exist at all. Present results

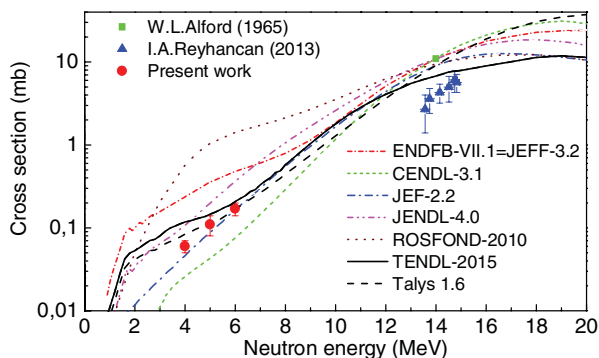


Figure 5. Present cross sections of the $^{144}\text{Sm}(n,\alpha)^{141}\text{Nd}$ reaction compared with existing measurements and evaluations for neutron energy region from 1.0 to 8.0 MeV.

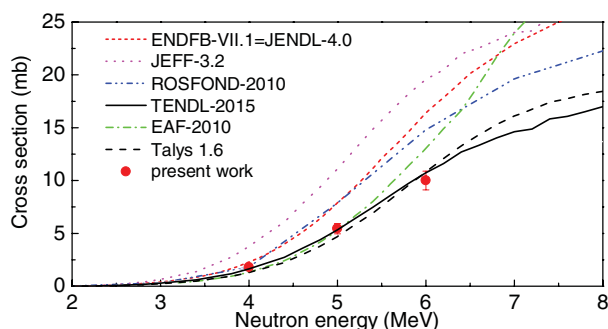


Figure 6. Present cross sections of the $^{66}\text{Zn}(n,\alpha)^{63}\text{Ni}$ reaction compared with existing measurements and evaluations for neutron energy region from 2.0 to 8.0 MeV.

at 4.0 and 5.0 MeV support the data of EAF-2010. In addition, our results agree well with the data of TENDL-2015. Further measurements at neutron energies from 8 to 12 MeV are also needed to clarify the discrepancies among different libraries.

4. Conclusions

In the present work, cross sections for the $^{144}\text{Sm}(n,\alpha)^{141}\text{Nd}$ and $^{66}\text{Zn}(n,\alpha)^{63}\text{Ni}$ reactions are measured $E_n = 4.0, 5.0$ and 6.0 MeV. Our results are generally in agreement with TALYS-1.6 calculations. For the $^{144}\text{Sm}(n,\alpha)^{141}\text{Nd}$ reaction there are big disagreements among different evaluation libraries. Our measurements support the data of JEF-2.2 libraries. For the $^{66}\text{Zn}(n,\alpha)^{63}\text{Ni}$ reaction, no measurements exist for neutron energies from 0 to 20 MeV. Present results at 4.0 and 5.0 MeV support the data of EAF-2010, and good agreements are obtained between our results and those of TENDL-2015. Further measurements for both

the two reactions are needed at neutron energies from 8 to 12 MeV to clarify the discrepancies among different libraries.

The authors are indebted to the operation crew of the 4.5-MV Van de Graaff accelerator of Peking University. The present work was financially supported by the National Natural Science Foundation of China (11175005 and 11475007).

References

- [1] M.B. Chadwick, E. Dupont, E. Bauge, et al., Nuclear Data Sheets **118**, 1 (2014)
- [2] EXFOR: Experimental Nuclear Reaction Data, database version of September 02, 2015, <https://www-nds.iaea.org/exfor/exfor.htm>
- [3] ENDF: Evaluated Nuclear Data File, database version of September 02, 2014, <https://www-nds.iaea.org/exfor/endl.htm>
- [4] Guohui Zhang, Yu.M. Gledenov, G. Khuukhenkhuu, M.V. Sedysheva, P.J. Szalanski, P.E. Koehler, Y.N. Voronov, J. Liu, X. Liu, J. Han, J. Chen, Physical Review Letters **107**, 252502 (2011)
- [5] Guohui Zhang, Rongtai Cao, Jinxiang Chen, Guoyou Tang, Yu.M. Gledenov, M.V. Sedysheva, G. Khuukhenkhuu, Nuclear Science and Engineering **156**, 115 (2007)
- [6] Guohui Zhang, Yu.M. Gledenov, G. Khuukhenkhuu, M.V. Sedysheva, P.J. Szalanski, Jiaming Liu, Hao Wu, Xiang Liu, Jinxiang Chen, V.A. Stolupin, Physical Review C **82**, 054619 (2010)
- [7] X. Zhang, Z. Chen, Y. Chen, J. Yuan, G. Tang, G. Zhang, J. Chen, Y.M. Gledenov, G. Khuukhenkhuu, M.V. Sedysheva, Physical Review C **61**, 054607 (2000)
- [8] Guohui Zhang, Hao Wu, Jianguo Zhang, Jiaming Liu, Yu.M. Gledenov, M.V. Sedysheva, G. Khuukhenkhuu, P.J. Szalanski, Eur. Phys. J. A **43**, 1 (2010)
- [9] Yu.M. Gledenov, M.V. Sedysheva, V.A. Stolupin, Guohui Zhang, Jinhua Han, Zhimin Wang, Xiao Fan, Xiang Liu, Jinxiang Chen, G. Khuukhenkhuu, P.J. Szalanski, Physical Review C **89**, 064607 (2014)
- [10] J.F. Ziegler, SRIM-2013, <http://www.srim.org/#SRIM>
- [11] A.J. Koning, S. Hilaire, and M.C. Duijvestijn, 0 "TALYS-1.0", *Proceedings of the International Conference on Nuclear Data for Science and Technology*, April 22–27, 2007, Nice, France, editors O. Bersillon, F. Gunsing, E. Bauge, R. Jacqmin, S. Leray, EDP Sciences, 2008, p. 211–214